Ref. Ares(2023)2082972 - 22/03/2023

D1.1. System Specifications and Requirements for Electric and Electronic Systems including Thermal Management System

Reinventing High-performance pOwer converters for heavy-Duty electric trAnSport

Grant Agreement Number 101056896

Deliverable name:	D1.1 System specifications and requirements for electric and electronic system including thermal management system
Deliverable number:	1.1
Deliverable type:	R
Work Package:	WP1: System specifications; components and materials. Ecodesign considerations.
Lead beneficiary:	VALEO EMBRAYAGES / VALEO EAUTOMOTIVE
Contact person:	David Lumbreras (david.lumbreras@upc.edu)
Dissemination Level:	PU
Due date for deliverable:	January 31, 2023

Funded by the European Union

Funded by the European Union. Views and opinions expressed are however those of the author(s) only and do not necessarily reflect those of the European Union or CINEA. Neither the European Union nor the granting authority can be held responsible for them.

DOCUMENT CONTROL PAGE

Author(s):	David Lumbreras
Contributor(s):	Arame Diop, Corneliu Barbu, Akash Kadechkar
Reviewer(s):	Arame Diop, Markus Koller
Version number:	v.5 M9
Contractual delivery date:	31 – 01 – 2023
Actual delivery date:	31 – 01 – 2023
Status:	Submitted

REVISION HISTORY

Version	Date	Author/Reviewer	Notes
v.0	07 – 12 – 2022	David Lumbreras (UPC)	Creation, First Draft
v.1	06 – 10 – 2022	David Lumbreras (UPC)	Working version almost consolidated
v.2	14 – 10 – 2022	Akrama Khan / Corneliu Barbu / Uffe Jakobsen / (AU)	Inclusion of thermal specifications
v.3	17 – 10 – 2022	David Lumbreras (UPC)	Consolidated version / Ready for review
v.4	21 – 10 – 2022	Arame Diop (VAL)	Add truck application and electro mechanic specifications. Reviewed
v.5	24 – 10 – 2022	Jose Sáez (NION)	Reviewed
v.6	28 – 10 – 2022	Luis Romeral (UPC)	Final version submitted
v.0 M9	21 – 12 – 2022	Arame Diop (VAL)	M9 upgrade. Completion of electromechanical specifications.
v.1 M9	23 – 12 – 2022	David Lumbreras (UPC)	Fulfilment of electronic specifications
v.2 M9	13 – 01 – 2023	Corneliu Barbu (AU) / Akash Kadechkar (NION)	Completion of thermal specifications and supervisory and monitoring systems specifications
v.3 M9	16 – 01 – 2023	David Lumbreras (UPC)	Consolidated version / Ready for review
v.4 M9	23 – 01 – 2023	Arame Diop (VAL) / Markus Koller (AIT)	Reviewed
v.5 M9	31 – 01 - 2023	Luis Romeral (UPC)	Final version submitted

ACKNOWLEDGEMENTS

The work described in this publication was subsidised by Horizon Europe (HORIZON) framework through the Grant Agreement Number 101056896.

DISCLAIMER

EXECUTIVE SUMMARY

The deliverable details the system specifications and requirements for the electric, electronic, and thermal management system of the powertrain. The deliverable also details the different protections of the converter, as well as the supervision and monitoring strategies. The specifications detailed in this deliverable update those defined in M6.

The power converter is going to be a three-level, three-phase, modular T-type converter based on SiC and GaN semiconductors. The converter, which will be installed on top of the motor, must be compact to ensure the gravimetric and volumetric power densities declared. The volume of the converter and the various components of the IMD are detailed in this deliverable.

The deliverable details the different semiconductors suitable to build the converter. Commercially available GaN devices withstand very low voltages and currents. Therefore, the document proposes two alternative strategies to solve this problem. One of the strategies is to use prototype GaN packs. Another strategy is to use several GaN transistors in parallel. The document presents a roadmap with alternatives to solve other possible problems. In addition, the document details the supervision and monitoring strategies that the converter will incorporate, as well as the different functions in the cloud.

Moreover, the document deals with the thermal management system. The environmental conditions in which the converter and motor can be used are presented and discussed. Furthermore, the deliverable presents the specifications of the proposed cooling system. Finally, the report concludes with a summary of the converter specifications.

TABLE OF CONTENTS

LIST OF FIGURES

LIST OF TABLES

1 INTRODUCTION

1.1 DESCRIPTION OF THE DOCUMENT AND PURSUE

This report describes the RHODaS specifications. More specifically, the report defines the electro-mechanic, electronic and thermal system specifications, as well as the final prototypes to be developed throughout the project.

The electro-mechanic system includes the electric motor and the gearbox. The electronic system comprises the wide-bandgap power converter, and the sensors and communication drivers for control, protections and monitoring. Finally, the thermal system includes the heatsink, the cooling system, and the thermal interface materials. Figure 1.1 illustrates the different systems and their main parts.

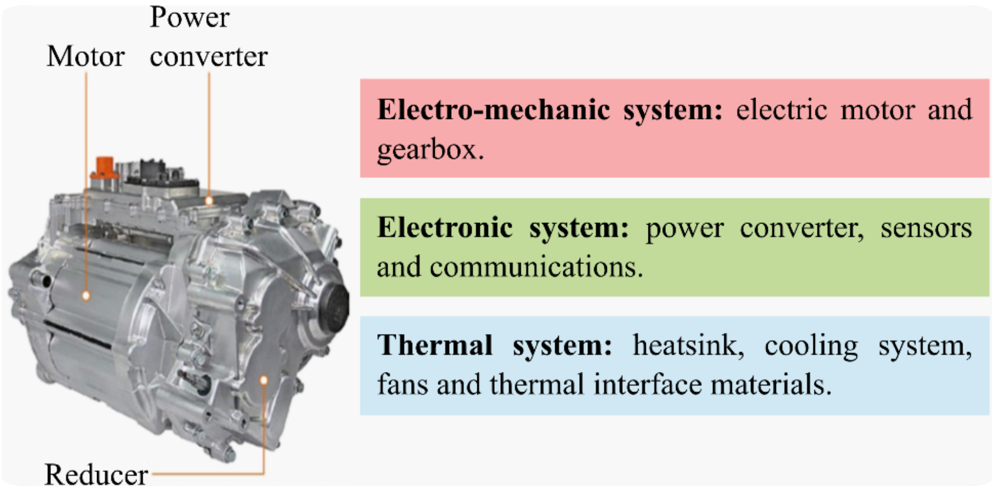

Figure 1.1 Overview of the different systems and their parts

The purpose of this document is to define the requirements and specifications for each of the before-mentioned systems. These requirements and specifications may be revised and updated according to the results obtained in WP2, WP3 and WP4.

1.2 WPS AND TASKS RELATED WITH THE DELIVERABLE

This deliverable refers to Task 1.1 and Task 1.2 included in WP1: System specifications; components and materials. Ecodesign considerations.

2 ELECTROMECHANICAL SPECIFICATIONS

This section describes the electromechanical requirements of the project, i.e., the characteristics of the motor and the dimensions of the power converter. It also describes the requirements for the gearbox system in order to fulfil truck application target. The power converter controls the engine. Hence, the electric motor imposes some converter characteristics, such as output voltages and currents.

Table 2.1 describes the requirements of the motor, vehicle and gearbox. The engine can operate with a maximum power of 250 kW. However, its rated power is 150 kW. Therefore, the inverter must be able to supply the latter power continuously. Additionally, the inverter must control the speed of the motor, which can be 10500 rpm maximum. This requirement will be achieved by an appropriate design of the converter control loop and its different sensors.

Table 2.1. Motor, vehicle and gearbox specifications

Subsystem	Parameter	Value
Motor	Max. Speed	10500 rpm
	Max. Torque	499 Nm
	Continuous Torque	228 Nm
	Rated power	150 kW
	Max. Power	250 kW
	Line voltage (rms)	700 V
	Motor maximal temperature: (Class H)	180°
	Maximal ambient temperature	From -20ºC to 50ºC
	Power factor (Cos Phi) @ continuous performance	[223 Nm, 4400 rpm]: 0.9132 [95 Nm, 10500 rpm]: 0.8177
	Durability	500 hours
Vehicle	Truck mass range	12T – 16T
	Max. Vehicle Speed	90 km/h
	Peak startability slope (30s)	16%
	Continuous startability slope	10%
Gearbox	Number of gear ratio	2
	1^{st} ratio (gearbox + differential)	38.9
	2^{nd} ratio (gearbox + differential)	21
	Differential ratio	2.71

The converter designed in the RHODaS has to operate continuously at the rated motor power (150 kW). Section 2 details that the proposed voltage for the DC Bus is higher than the current voltage. Consequently, the electrical isolation and gearbox of the motor should be modified to operate at these higher voltages. Higher voltages in the DC system mean less current, less copper, less weight and less cost, for the same power. A 1000-volt system in the DC Bus has the added advantage of reducing the motor mass too, because it allows the motor to run at higher speed, then increasing the power density.

In addition, the motor also determines the shape of the converter. The power converter will be placed on top of the engine and connected with short cables, as shown in Figure 1.1. Hence, the engine housing will be modified to integrate the converter. Table 2.2 details the engine dimensions.

Table 2.2. Motor dimensions

Machine size	Stator	Rotor
Outer diameter	240 mm	168.1 mm
Active length	110 mm	110 mm
Air gap	0.95 mm	

2.1 VEHICLE TARGET

With these electric machine specifications, truck application target for RHODaS project will be N3 category with a maximum mass between 12 and 16 tonnes. Table 2.1 describes the user requirement (at wheel) and the related two speeds gearbox in order to respect requirements.

With these specifications, the overall powertrain dimensions (power converter + electric machine + gearbox) can be calculated. Table 2.3 and Figure 2.1 show the preliminary powertrain dimensions. Note that this is a first estimation since the final measures of the power converter will depend on the final components, the geometry, the thermal system, etc. Section 3 presents calculations on the converter dimensions from a thermal point of view. The final dimensions of the converter, IMD and integrated system specifications shall be performed in Task T5.5 and presented in D5.4 (M42), as detailed in the DoA.

Table 2.3. Preliminary powertrain dimensions

	X (length) (mm)	Y (height) (mm)	Z (width) (mm)
Overall powertrain	1790 max.	600 max.	600 max.(1)
Electric Motor	400 max.	380(2)	380(2)
Power Converter	210 max.(3)	30 max.(2)	380 min.(4)
Gearbox	590 max.	410 max.	595 max.
Differential	800 max.(5)	600 max.(5)	600 max.(5)

(1) ⇒ without the side shafts.
(2) ⇒ linked and limited by the gearbox max height.
(3) ⇒ limited by the proposed height width and expected power density (100 kW/L).
(4) ⇒ limited by the gearbox max. width.
(5) ⇒ based on conventional differential.

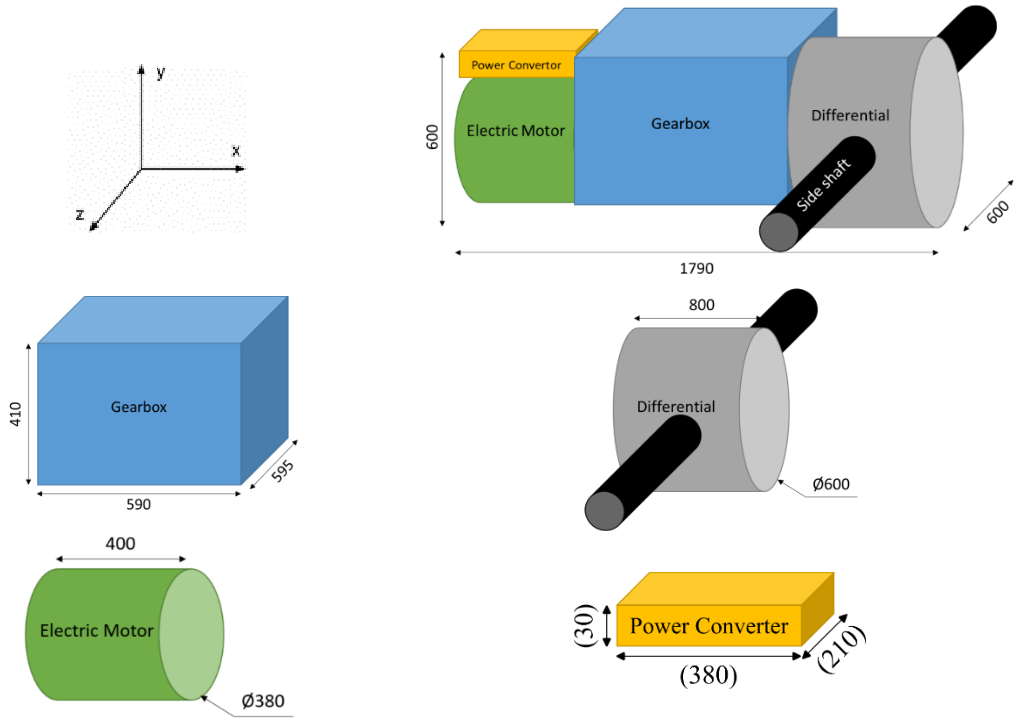

Figure 2.1 Preliminary dimensions of the IMD and its different parts

The RHODaS project will develop an electric powertrain consisting of the electric motor and the power converter. To test the technology, this powertrain can be connected to a mechanical gearbox and differential to build a complete IMD like the one depicted in Figure 2.1.

The reference values to establish the tests and objectives to be achieved with this IMD can be obtained from standard driving cycles.

Driving cycles are calculated using the Vehicle Energy Consumption Calculation Tool (VECTO). VECTO is a simulation tool developed by the European Commission. The tool allows us to determine CO2 emissions and Fuel Consumption from Heavy Duty Vehicles (trucks, buses and coaches) with a Gross Vehicle Weight above 3500 kg. In this case, the axle configuration is a 4x2 (four wheels with two driving wheels). Applicable driving cycles are the urban and regional driving cycles (see Figure 2.2).

Lorry Segmentation (Table 1 of Annex I to Commission Regulation (EU) 2017/2400)

Elements relevant to the classification in vehicle groups			Vehicle group	Allocation of mission profile and vehicle configuration							Standard body allocation
Axle configuration	Chassis configuration	Technically permissible max. laden mass (tons)		Long haul	Long haul (EMS*)	Regional delivery	Regional delivery (EMS*)	Urban delivery	Municipal utility	Construction	
4x2	Rigid	>3.5 – <7.5	(0)	*not covered yet*							
4x2	Rigid (or tractor)**	7.5 – 10	**1**			R		R			B1
4x2	Rigid (or tractor)**	>10 – 12	**2**	R+T1		R		R			B2
4x2	Rigid (or tractor)**	>12 – 16	**3**			R		R			B3
4x2	Rigid	>16	**4**	R+T2		R			R		B4
4x2	Tractor	>16	**5**	T+ST	T+ST+T2	T+ST	T+ST+T2				
4x4	Rigid	7.5 – 16	(6)	*not covered yet*							
4x4	Rigid	>16	(7)	*not covered yet*							
4x4	Tractor	>16	(8)	*not covered yet*							
6x2	Rigid	all weights	**9**	R+T2	R+D+ST	R	R+D+ST		R		B5
6x2	Tractor	all weights	**10**	T+ST	T+ST+T2	T+ST	T+ST+T2				
6x4	Rigid	all weights	**11**	R+T2	R+D+ST	R	R+D+ST		R	R	B5
6x4	Tractor	all weights	**12**	T+ST	T+ST+T2	T+ST	T+ST+T2			R	
6x6	Rigid	all weights	(13)	*not covered yet*							
6x6	Tractor	all weights	(14)	*not covered yet*							
8x2	Rigid	all weights	(15)	*not covered yet*							
8x4	Rigid	all weights	**16**							R	(generic weight+ CdxA)
8x6 8x8	Rigid	all weights	(17)	*not covered yet*							

* EMS - European Modular System
** in these vehicle classes tractors are treated as rigids but with specific curb weight of tractor
T…Tractor
R… Rigid & standard body
T1,T2… Standard trailers
ST…Standard semitrailer
D… Standard dolly

20

European Commission

Figure 2.2 Vehicle target

The mission profiles are taken from VECTO. At this moment, VECTO can handle only trucks with a thermal engine. Therefore, a truck of 16T is used for the simulation. The thermal engine used has the nearest power as RHODaS's EM continuous power.

Figure 2.3 and Figure 2.4 show the two mission profiles. Figure 2.3 shows the driving profile in an urban environment. This profile exhibits many acceleration and deceleration phases. This behaviour is especially interesting for an electric vehicle, since it allows for more regenerative braking phases. Figure 2.4 plots a regional mission profile. This profile has fewer acceleration and deceleration phases. In addition, it has more constant high-speed phases.

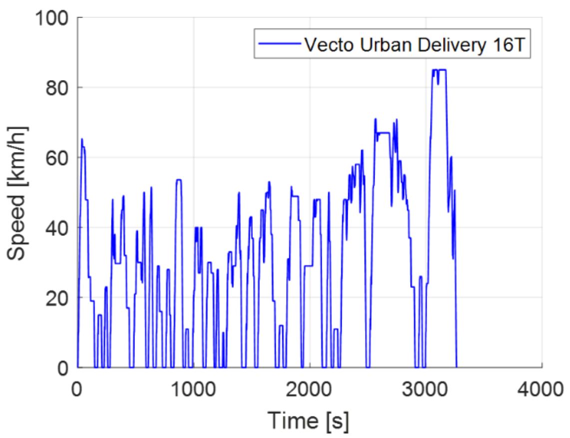

Duration (s)	3263
Distance (Km)	28
Max Speed (Km/h)	85
Average Speed (Km/h)	30
Max Acceleration (m/s²)	1

Figure 2.3 VECTO mission profile: urban delivery

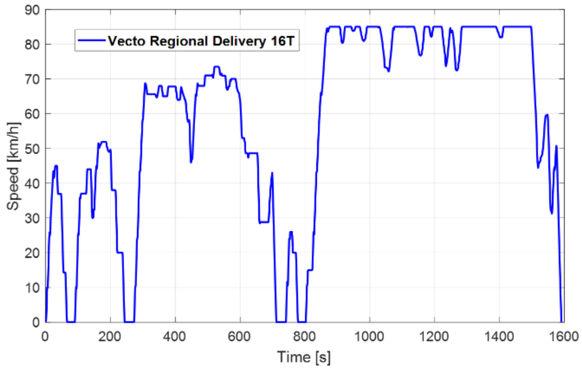

Duration (s)	1591
Distance (Km)	26
Max Speed (Km/h)	85
Average Speed (Km/h)	58.4
Max Acceleration (m/s²)	1

Figure 2.4 VECTO mission profile: regional delivery

Once the IMD target is set, the overall requirements (functionalities) will be discussed in the next paragraphs. The requirements can be divided in two parts:

- The operational requirements, also known as the main functions, describe the purpose of the system (the IMD or eTruck). They indicate the operations that the system should do;
- The non-operational requirements describe the qualities that the product should have. It covers regulations, dependability, constraints, etc.

The final goal of this project is to develop and test the innovative power converters within a powertrain in test bench. Therefore, the final stage of this study will be a test bench. Different tests will be realized to validate, through several test standards, the operability of the whole system. The specific tests to be performed in the IMD shall be defined during task T5.1.

2.2 OPERATIONAL REQUIREMENTS

The main missions of the IMD system are:

- To provide mechanical power to the wheel according to a VCU request
- To provide electric power from wheel according to a VCU request
- To dissipate heat according to a set point
- To provide information to other systems

Based on the EM power and the 2-speed gearbox, the final power available at wheel are shown in Figure 2.5. Depending on the considered gear, two-wheel power curves are available. Power profiles of the first ratio are in blue while those of the second ratio are in red. The power profiles of the first gear allow to reach continuous and maximal startabilities while those of the second gear one allows to reach the maximal speed.

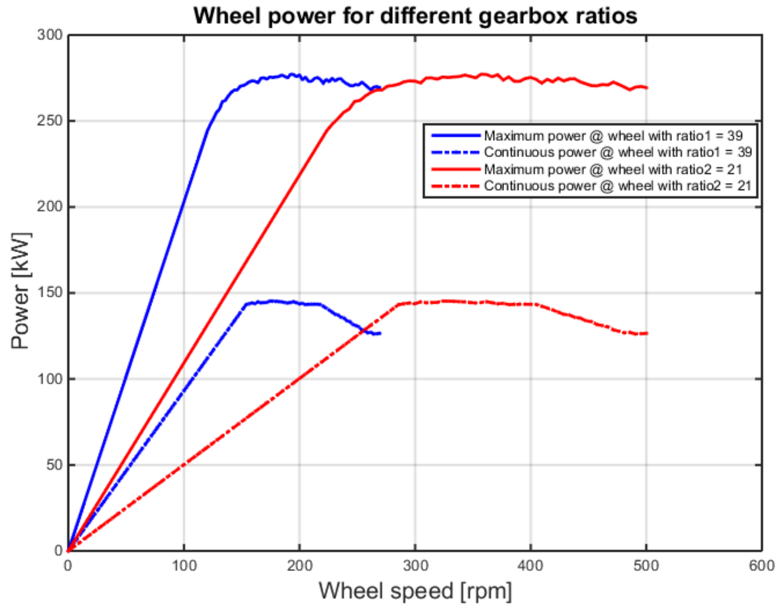

Figure 2.5 Truck wheel power

The IMD will interact with several subsystems during operation and testing. Therefore, the IMD must be designed for proper interaction with:

- Low-voltage network: which gives power to the electronic control unit of the system
- High-voltage network: provide/receive power to/from the IMD
- Load machines: which will simulate the vehicles wheels
- Test bench chassis: to support mechanically the system
- Bench VCU: to simulate one part of the VCU on vehicle

Figure 2.6 summarizes the interactions described above.

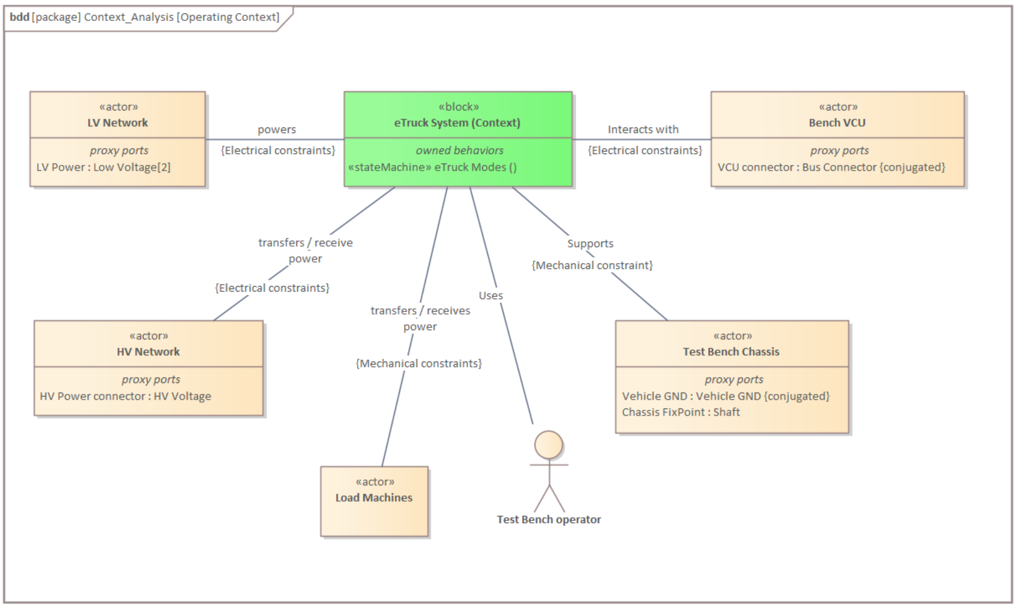

Figure 2.6 Test Bench operating context

2.3 NON-OPERATIONAL REQUIREMENTS

Non-operational functionalities are overall qualities and constraints that the system has to respect. Those of the eTruck system are the following:

- Must resist to chemical environment
- Must resist to climatic conditions
- Must resist to EMC perturbation
- Must limit EMC perturbation
- Must resist to mechanical environment
- Limit mechanical environment perturbation (NVH)

These constrains will be totally defined in upcoming tasks (T1.4) and deliverables (D1.2).

3 ELECTRONIC SPECIFICATIONS

This section describes the electronic specifications of the designed power converter. One of the objectives of the RHODaS project is to develop a multilevel T-type converter.

This converter topology has a particular feature: the transistors must withstand different voltages. Figure 3.1 shows a three-level T-type converter. The top and bottom transistors –S_{x1} & S_{x4}– withstand the full DC bus voltage. Nevertheless, the transistors connected to the midpoint of the bus –S_{x2} & S_{x3}– only withstand half of the bus voltage.

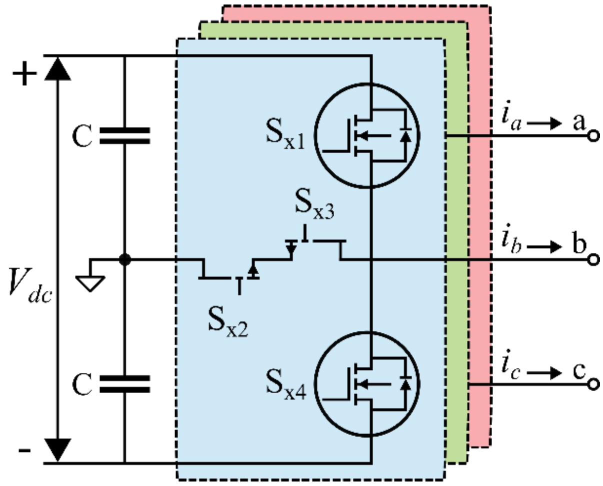

Figure 3.1. Three-level T-type power converter

This uneven distribution of voltages is of great importance when choosing semiconductors. Two proposals are presented in this project, for low-power and high-power converters, respectively: working with an 800 V DC bus voltage or with a 1000 V DC. Section 3 further discusses this matter.

Regardless of the converter topology used, the converter must meet some requirements. First, it must use a combination of silicon carbide (SiC) and gallium nitride (GaN) in order to achieve peak efficiencies above 98%. Second, the high-power converter must provide a line voltage of 640 V minimum to drive the motor. Therefore, the DC bus must operate at a minimum voltage of 900 V, with 1000 V being the desirable voltage.

Increasing the bus voltage can reduce the operating current without affecting the total power of the converter, which must have a power rating of 150 kW independently of the DC bus voltage. The DC bus voltage also influences the dv/dt. This parameter will be analysed and mitigated if it causes problems. Possible mitigation strategies may be the design of specific transistor gate circuit, the use of passive filters or the increment of the motor isolation.

In addition, this converter has to have a switching frequency between 50 and 100 kHz. Increasing the switching frequency increases the losses and electromagnetic emissions (EMI). Nevertheless, it improves the quality of the current at the converter output. The converter should have lower losses and EMI than a standard two-level converter. Therefore, the switching frequency must be selected to reach a balance between losses, EMI and current quality (i.e., harmonics and Total Harmonic Distortion, THD), although it may have a variable range depending on the operating conditions of the converter to optimize a certain criterion.

3.1 CONVERTER TOPOLOGIES

As mentioned before, three-level T-type converters exhibit an uneven voltage distribution. The top and bottom transistors withstand the full DC voltage, while the other transistors only withstand half of the voltage. Consequently, the DC bus voltage heavily influences the selection of the semiconductors.

Before determining the converter topology, it is necessary to comprehend which semiconductors are available on the market. GaN semiconductors are not as widespread as SiC in power electronics. Most commercial semiconductors withstand voltages up to 600 or 650 V. In addition, the current these semiconductors can withstand is usually low, up to 60 A.

Table 3.1 shows the GaN semiconductors that may be used in the RHODaS project. First, there are the GS66516T/B transistors. These transistors are commercially available and are manufactured by GaN Systems. Although they withstand voltages up to 650 V, their maximum current is low, about 60 A per device. If we decide to use these transistors, we should put several in parallel to increase the maximum current of the converter. However, using GaN transistors in parallel is complex, as non-optimal switching can occur due to inductances and other parasitic elements. Therefore, we propose to use two GaN transistors in parallel (see Figure 3.4). This solution also limits the maximum current of the converter, so control strategies will be adopted to solve this problem and to be able to work with all the maximum required power. These strategies are detailed in Section 3.3.

As detailed in the previous version of the deliverable (M6), some manufacturers produce 200 A GaN modules (ViSIC model V08TC65S1A2). However, these GaN are not commercially widespread, their information is limited, and we have not obtained a response from the manufacturer.

Secondly, the companies Amosense and GaN Systems are manufacturing GaN power modules. These modules are not commercially available. However, GaN Systems is part of the IAB of the project, and they are interested in providing us with these modules, if possible. The modules withstand voltages and currents up to 650 V and 200 A, respectively. This solution would extend the working range of GaN transistors. However, these modules contain a half-bridge structure, while T-type converters use two opposite transistors in the middle point. According to GaN Systems, they will try to provide us with a specific module for the T-type converters. Otherwise, we may use two antiparallel modules.

Table 3.1. Possible GaN devices

Reference	**Manufacturer**	**Topology**	**V_{DC} (V)**	**I_{DS}(A)**
GS66516T GS66516B	GaN Systems	e-HEMT (discrete)	650	47 (T_c=100 ºC)
---	Amosense + Gan Systems	GaN Power Module (Prototype)	650	200 (T_c=25 ºC)

SiC is a much more mature technology than GaN in power electronics. Consequently, there are more commercially available SiC devices. These transistors can withstand high voltages and currents. Table 3.2 details different commercially available SiC transistors that may be used in the power converter.

Table 3.2. Commercially available SiC devices

Reference	Manufacturer	Topology	V_{DC} (V)	I_{DS}(A)
MSCSM170AM039CT6AG	MICROCHIP	Half-bridge	1700 V	416 (Tc=80 ºC)
MSCSM120AM042CT6LIAG	MICROCHIP	Half-bridge	1200 V	394 (Tc=80 ºC)
NVVR26A120M1WSS	ONSEMI	Half-bridge	1200 V	400 (Tc=175 ºC)

The previous analysis shows that GaN semiconductors are only available for low-voltage applications (650 V at maximum). For 1000 V DC-link voltage, the safety margin for GaN could not be sufficient due to suboptimal commutation loop, SiC device packaging, and additional Q_{rr} from SiC MOSFETs. Hence, GaN devices can restrict the maximum DC bus voltage. Therefore, it may be necessary to lower the bus voltage slightly to around 900 or 950 V. This is discussed in more detail in Section 3.2.

Figure 3.2 shows the proposed GaN-SiC T-type converter. This converter uses a combination of SiC and GaN. The SiC devices withstand the full bus voltage, while the GaN devices only withstand half. Therefore, the bus voltage can be 1000 V. Thus, the GaN transistors would withstand 500 V, so there is a little safety margin.

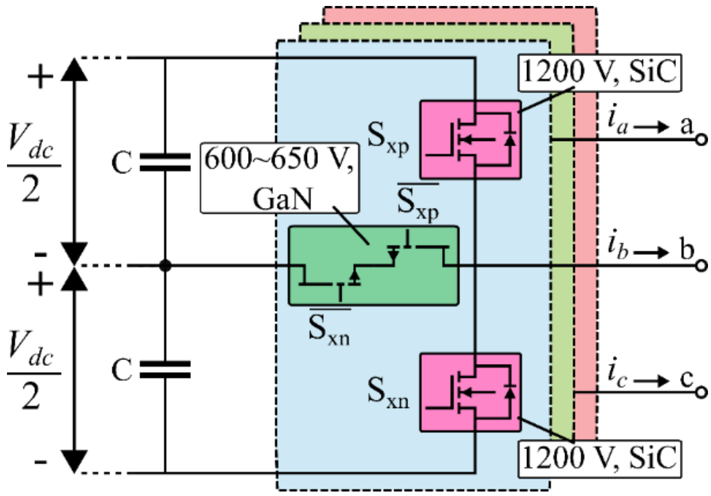

Figure 3.2. Hybrid GaN-SiC T-type power converter.

This topology will be used in the intermediate prototype. Hence, it will work with low currents and will be used to verify control, modulation, and study EMI and losses. The results obtained in this converter will be used to design the high-voltage converter.

Furthermore, this topology should also be the topology of the final converter. However, it is necessary to examine alternative topologies due to the previously mentioned problems. These alternative topologies are defined in Section 3.2.

3.2 ROADMAP

As discussed above, commercially available GaN devices can only withstand low voltages and currents. Therefore, it is necessary to define alternatives to the GaN-SiC hybrid converter initially proposed. Figure 3.3 shows the roadmap of the designed converter.

If the GaN e-HEMTs cannot withstand the bus voltage, the voltage shall be reduced to 900 or 950 V. If GaN devices cannot withstand the currents needed to drive the motor, there are some alternatives. Firstly, the central part of the converter, i.e., the GaN transistors, can be parallelised (Figure 3.4). This solution significantly reduces the current through each of the GaN transistors. In addition, this option does not over-complicate the design of the converter and does not require many additional components. Secondly, the converter may include several modules in parallel (Figure 3.5).

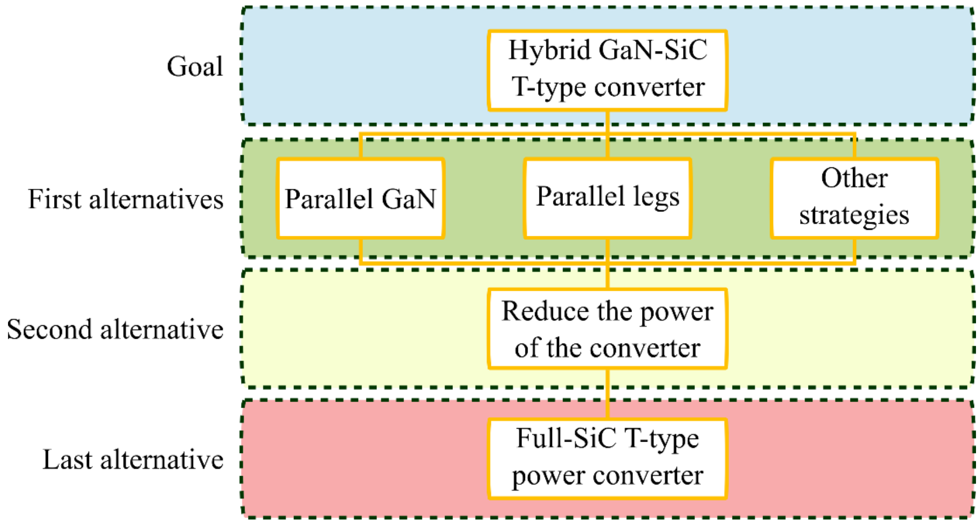

Figure 3.3. Proposed roadmap

However, this solution would significantly increase the cost of the converter and also its volume due to the number of additional components required. Moreover, it complicates the modulation technique and also control algorithm. Finally, other strategies can be used. For example, control and modulation algorithms can be designed to reduce the currents through the GaN transistors.

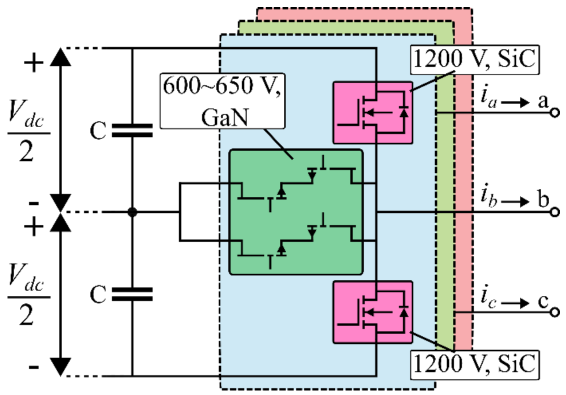

Figure 3.4. Hybrid T-type power converter with parallel GaN devices

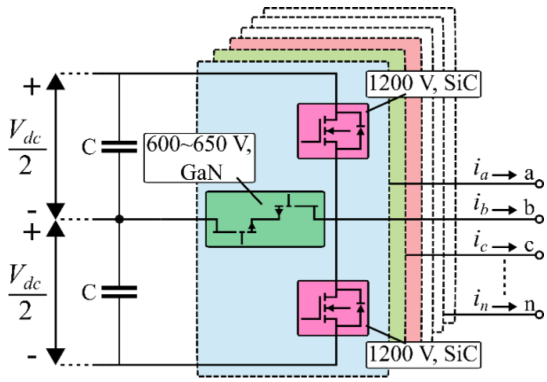

Figure 3.5. Hybrid T-type power converter with parallel legs

If none of the above strategies is possible, the power of the designed converter will be reduced. This solution involves lowering the power to bring the GaN transistors to their performance limit.

Finally, a full-SiC converter is proposed as the ultimate risk-mitigation solution (Figure 3.6). The Full-SiC converter will only be built if it is demonstrated that the project objectives cannot be achieved in any way with GaN.

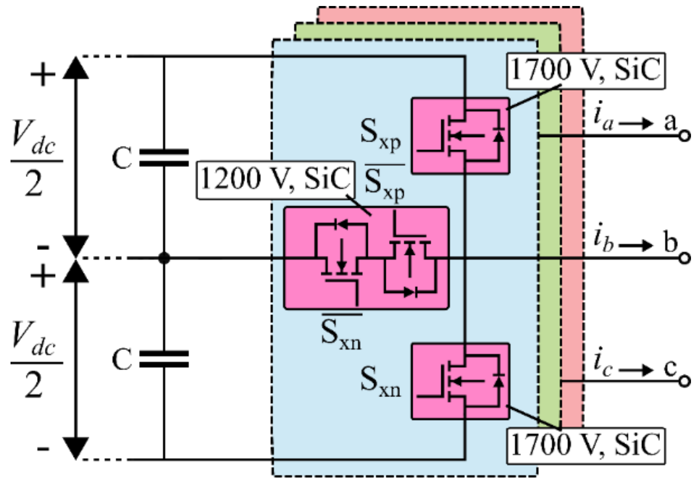

Figure 3.6. Full-SiC T-type power converter

3.3 CONTROL SPECIFICATIONS

The control of the converter shall be specific to the designed T-type converter. As discussed above, one of the limitations of the converter is the use of GaN semiconductors. These semiconductors withstand low voltages and currents, so the control should mitigate this problem.

The power converter will have two modes of operation: standard (Figure 3.7) and high-duty (Figure 3.8).

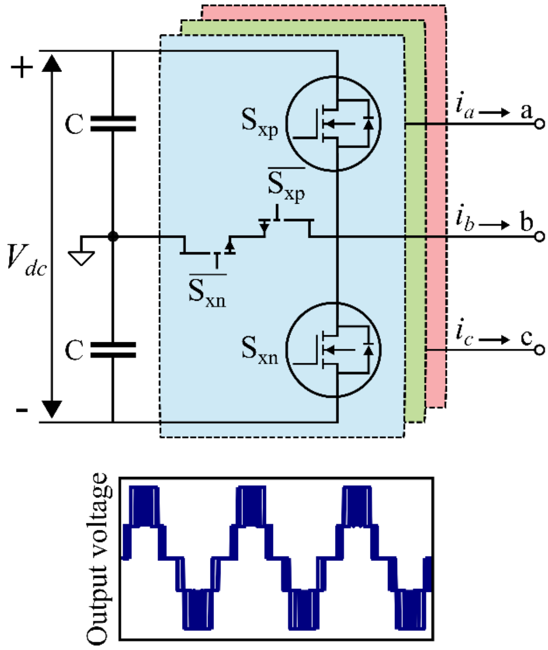

Figure 3.7. Standard operation mode

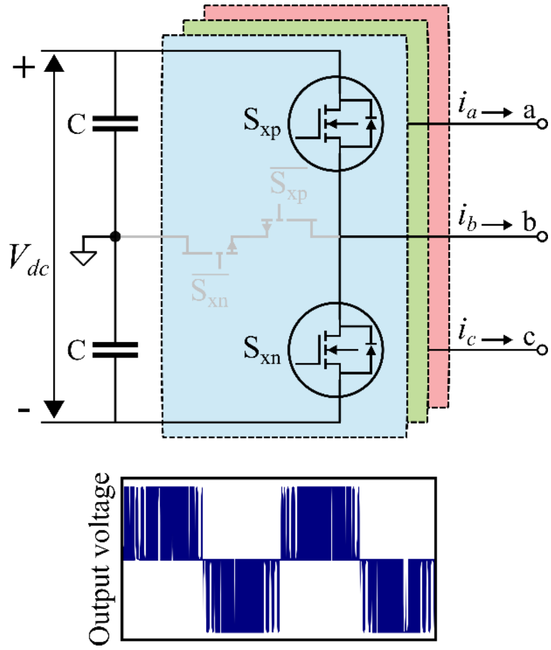

Figure 3.8. High-duty operation mode

In the standard operation, all transistors are working. Therefore, the converter provides three voltage levels at the output. This operation mode improves the quality of the output currents and reduces electromagnetic emissions. However, the maximum power of the converter is limited by the maximum current that the GaN transistors can withstand.

In high-duty operation, only the SiC transistors switch, i.e., the GaN transistors remain open. Consequently, the output voltages have only two levels. Hence, the quality of the output currents and the electromagnetic emissions are worse. However, SiC transistors withstand higher currents than GaN transistors. Therefore, this operation mode is particularly suitable when the converter has to deliver high power.

The control should change the mode of operation from standard to heavy-duty and vice versa without stopping the power converter. The converter shall be able to operate in standard mode by default and switch to heavy-duty operation when the currents required by the motor are significantly high.

Moreover, the control of the converter has requirements independent of the converter topology used. The main requirements are twofold: fault tolerance and loss reduction.

The converter must be fault-tolerant. If one of the transistors fails, the converter must be able to continue to operate normally. This objective may be achieved with high-duty operation. GaN transistors are usually the most fragile, so if one fails, the converter will switch to operate only with SiC devices, i.e., in heavy-duty mode. Adding the fourth phase can also be useful to achieve higher fault tolerance. However, this solution is discarded in the high-power converter, as it would compromise the size and power density of the final converter.

In addition, the designed converter should have lower losses than currently available converters. The control can achieve this goal by reducing the switching of the transistors, either by clamping them or by varying the switching frequency. These methods typically reduce electromagnetic emissions (EMI), so an improvement in this area is expected.

Finally, the controller may perform other functions, such as balancing the DC bus capacitors' voltages.

Many of these solutions will be investigated on the low power converter, which will serve as a test bed for research and development.

Table 3.3 summarizes the electronic specifications detailed in this section for the power converter. Table 3.3 includes the specifications for the test converter as well as the high-power converter. Moreover, Appendix A contains detailed calculations to find some of the converter parameters.

Table 3.3. Summary of the electronic specifications

Parameter	**Test converter (low-power)**	**Power converter (high-power)**
Maximum efficiency	> 97 %	> 97 %
DC bus voltage	800 V	1000 V
Rated power	10 kW	150 kW
Maximum power	15 kW	250 kW
Semiconductor	GaN + SiC	GaN + SiC
Switching frequency	50 – 100 kHz	50 – 100 kHz
Motor line voltage	640 V	700 V
Rated current (rms)	12 A	150 A
Maximum current (rms)	18.75 A	250 A

3.4 LOCAL PROTECTIONS

The converter is going to have several protections to ensure its correct operation and to protect it against unforeseen events. These protections are as follows:

- **Overvoltage protection:** the inverter will stop when an overvoltage is detected.
- **Overcurrent protection:** the converter will operate in high-duty mode when it detects that it must deliver currents higher than the GaN can withstand. The converter will stop when it detects currents higher than the SiC can resist.
- **Over-temperature protection:** the converter will stop operating when the temperature of the converter is excessively high.
- **Protection against unbalance on the DC bus:** by default, the control shall balance the DC bus. The converter shall stop operating or switch to high-duty operation if the DC bus capacitors become significantly unbalanced.
- **Emergency stop:** the converter shall have an emergency stop function to avoid dangerous situations that may occur or are occurring imminently. The emergency stop function must be available and operational at all times, regardless of the

operating mode. The emergency stop device is a back-up to other safeguarding measures and not a substitute for them.

All functions involving the stop of the converter shall maintain the stop command. That command must be sustained by the engagement of the device until that engagement is specifically overridden. It must not be possible to engage the device without triggering a stop command. It must be possible to disengage the device only by an appropriate operation, and disengaging the device must not restart the power converter but only permit restarting.

In addition to the above protections, the converter may include additional protections for the drivers. These protections can be using two inputs to mitigate crosstalk and a Miller clamp to avoid false switching, among others. However, these driver functionalities will be fully defined at month 20, after finishing tasks T2.1, T2.2 and T2.3.

3.5 SUPERVISORY AND MONITORING SYSTEMS

This chapter covers the general architecture of the cloud-based software of the RHODAS project and therefore, according to its general objectives, this software will cover the following high-level requirements and goals:

- Develop effective software architectures (back-end) to allocate the different AI modules and the Digital Twin (DT).
- Provide an innovative service layer to allow the interaction with the DT and Decision Support System (DSS) in an interoperable IoT platform, for instance for smart EV industry.
- Apply Data Mining and Big Data for ensuring data quality and historical data traceability.
- Develop ergonomic Graphical User Interfaces (GUI) (front-end) to increase adoption, awareness, and user engagement.

3.5.1 GENERAL ARCHITECTURE DESCRIPTION

In the RHODAS project, the remote monitoring and supervisory system of the Integrated Motor Drive (IMD) powertrain is built using different cloud-based software platforms as highlighted in the general architecture shown in Figure 3.9.

The different cloud-based software platforms to be implemented in the RHODAS project are IoT Platform and Digital Twin Platform. The IoT platform (IOTP) is interfaced with the powertrain of the heavy-duty EV via IoT gateway, gathering all monitored data and storing it in its Big Data repository. The Digital Twin Platform (DTP) reads real data from the IOTP but is also in charge of producing data itself through the execution of AI algorithms, which will be stored in the IoT platform as well. The graphical user interface is also part of the IoT platform for the data visualization.

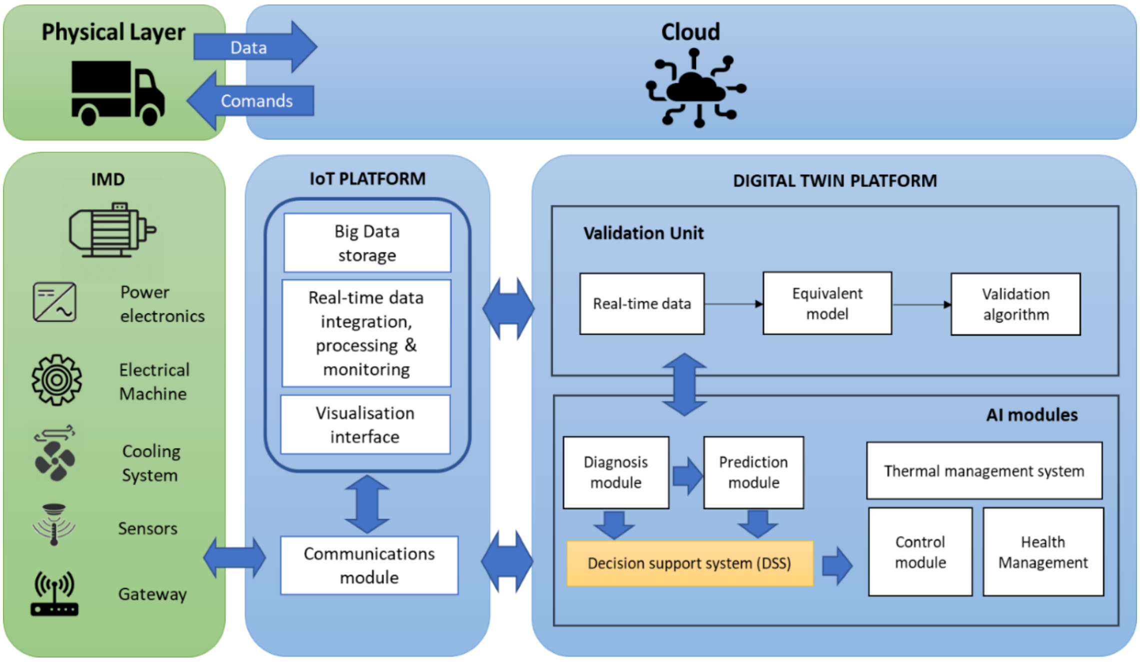

Figure 3.9. General Architecture of Rhodas software platforms.

3.5.2 IOT GATEWAY, INTERFACES AND COMMUNICATION PROTOCOLS

As shown in Figure 3.9, IoT Gateway is a physical device that acts as a direct connection point between the local intelligent devices (sensors/actuators) and the cloud-based platforms. In automotive industry, IoT Gateway is also known as Telemetry Control Unit (TCU) which is responsible for wirelessly connecting the vehicle to cloud services. In this project, IoT Gateway or the TCU installed in the heavy-duty EV powertrain demonstrator will collect data from the different control units such as Powertrain Control Module (PCM), and additional smart sensors (for digital twin features). CAN bus is the most used communication protocol in vehicles as it has proven to be a reliable bus system for fast data transfer between different Electronic Control Units (ECUs) of the vehicle like PCM, TCU, Human-Machine Interface (HMI), Body Control Unit (BCU), etc. However, to demonstrate the technology and considering that the IMD is not installed in an actual vehicle, any of the standard communication protocol, such as CAN, Modbus, Profinet, Ethernet, etc. can be used for the data transfer from the PCM and TMS to the IoT Gateway.

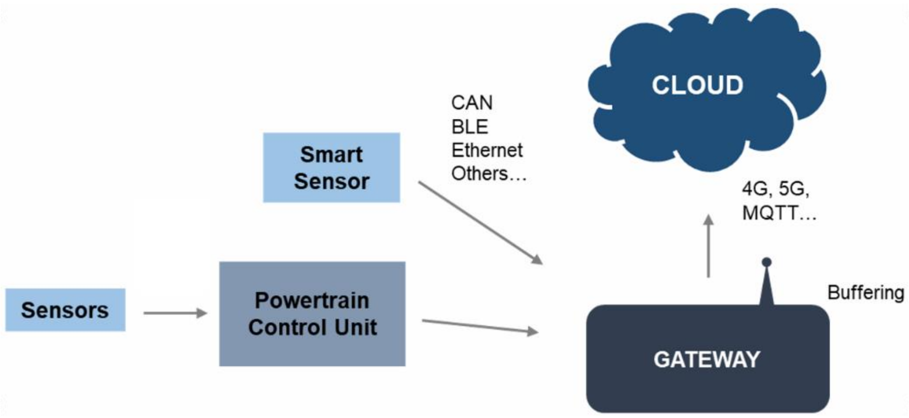

Figure 3.10. Basic diagram of IoT communications architecture.

Moreover, PCM will collect data from the sensors integrated in the different parts of the powertrain like the power converter, motor, transmission, etc. The sensors integrated within the thermal cooling system may send information to the PCM or to the gateway. The system will also include some additional smart sensors that will be useful to carry out the DT functions. These smart sensors will communicate directly with the IoT gateway via Bluetooth Low Energy (BLE), CAN or any other suitable communication protocol. The communication protocols to be used for data collection will be further described during task T1.5. and included in deliverable D1.4.

The IOTP is the front-line cloud-based platform in charge of communicating with vehicles through their communication IoT gateway. As mentioned, IoT gateway will gather data from the different systems of the powertrain like IMD, Thermal Management System, etc. in the vehicle through the agreed communication protocol and accumulate it in a buffer while, in time, it will be pushed up to the IOTP through 4G or 5G or any other wireless internet connections and the MQTT protocol, that proves to be more efficient, reliable, and secure in massive IoT data communications, also offering a low power consumption profile (see Figure 3.10). Finally, REST API interfaces will be used among the platforms since it is light and simple, relies on the HTTP standard, it is format-agnostic, and it makes clients and servers independent, offering a great scalability and flexibility. Custom-made JSON messages will be exchanged through secured endpoints and, when big amounts of data be required – for example to train data-based models residing in DTP – Python scripts will be enabled in the IOTP.

3.5.3 INTERNET OF THINGS PLATFORM (IOTP)

The IOTP is mostly a service layer which provides interconnection of the different entities such as software platforms like DTP in RHODAS, as well as other hardware systems, such as the IoT Gateway integrated in the EVs. The IoT architecture will allow real-time and secure interaction and cooperation between hardware and software elements in an intelligent and self-configuring approach, which will ensure continuous monitoring, protection, and improved performance of the RHODAS powertrain. At the same time, the front-end will be designed and shaped to the needs of the supervising users of the system. The IoT platform in RHODAS will be mainly implemented based on the software architecture of the datAssist™ platform developed by NVISION. The IoT platform will be developed in WP4 of RHODAS. Requirements for the IOTP are classified with the abbreviations shown in the following tables.

Table 3.4. Abbreviation for IOTP requirements.

Abbreviation	Module
BD	Big Data
UI	User Interface
GE	General requirements

The following tables describe the functional requirements (FR) for the IOTP:

Table 3.5. Functional general requirements for the IOTP.

GE-FR-XX	Description
GE-FR-01	Information status of the various modules will be maintained, which ones are running, and which ones are not
GE-FR-02	The status of the different modules will be monitored
GE-FR-03	Information and states from sensors in the powertrain will be processed in near-real time
GE-FR-04	The latest information and status of sensors will always be accessible
GE-FR-05	The configuration information of each sensor will be stored, including minimum and maximum thresholds for alerts, both warning and alarm levels
GE-FR-06	Information will be maintained on which sensors are connected and which are not
GE-FR-07	Be able to perform a single or massive load of sensor data
GE-FR-08	Be able to provide functions for consulting historical sensor information between established dates and times
GE-FR-09	Be able to provide functions for time aggregation of data

Table 3.6. Functional Big Data requirements for the IOTP.

BD-FR-XX	Description
BD-FR-01	Information communication will be done through JSON packages
BD-FR-02	The information packages will be of three types: control, states and data
BD-FR-03	Massive data capture from the gateways and interface modules
BD-FR-04	Data filtering and pre-processing to avoid useless information
BD-FR-05	Data fusion to produce more consistent, accurate and useful information
BD-FR-06	Big Data storage environment to supply fast access to data
BD-FR-07	Big Data models for data processing to ease data analysis
BD-FR-08	Algorithms for extracting on-line, historical, and predictive information of the powertrain
BD-FR-09	Simple alerts from monitored data will be triggered attending to minimum and maximum values for warning and alarm levels
BD-FR-10	AI/ML agents for powertrain management, for status, actions and recommendations

Table 3.7. Functional UI requirements for the IOTP.

UI-FR-XX	Description
UI-FR-01	A main graphical user interface screen will be shown with the operational information of the installation, displaying real- time status of sensors, while allowing to interact with actuators (if necessary)
UI-FR-02	A window in the main status screen will show last few actions, alerts and recommendations generated by the platform
UI-FR-03	At least, there will be one visualization level, but attending to the hierarchical structure of the powertrain components and the EV, a deeper multilevel visualization may be shown
UI-FR-04	Historical view of one or some of existing sensors in the same screen, allowing to select start and end date and time
UI-FR-05	Historical view of all automatic actions, alerts and recommendations generated by the platform, allowing to select start and end date and time
UI-FR-06	Be able to export all historical data in CSV format for further external analysis
UI-FR-07	Interface designed using UX design, attending to usefulness, easiness to use, and enjoyment to interact with
UI-FR-08	Interface designed using UI design, including an analysis of used colour patterns
UI-FR-09	Implement on-line and off-line modes; sensors will be read in both modes, but orders to actuators won't be sent during off-line mode
UI-FR-10	Be able to execute actions on connected devices based on user commands through the interface (if required)

3.5.4 DIGITAL TWIN PLATFORM (DTP)

The purpose of the DTP is to construct a digital replica of the powertrain which describes the physical powertrain in real-time. This includes collecting and processing data for remote protection and to improve the performance during operation, as well as to improve manufacturing, and LCA/LCC tools. In RHODAS, multi-scale models and advanced algorithms will be integrated into the DTP to optimize the overall efficiency of the powertrains. The DTP will be implemented in WP4 of RHODAS.

In RHODAS, the DTP consists of several software modules and digital tools for the implementation of the different remote features which are less vulnerable to latency. Moreover, the functional requirements will change from one feature to another. However, in general the historical data of the powertrain components could be used for the implementation of the digital twin features as mentioned below.

- **Condition Monitoring and Protection**: the current State of Health (SoH) of the IMD powertrain is estimated or computed using the sensor data acquired from the IMD powertrain. Correspondingly, a maintenance action is performed if an abnormal behaviour is detected or if the SoH falls below the minimum threshold. At the same time the software should be capable of handling fault tolerance by detecting faults in the sensors to avoid false alarms and to let the system run safely until the planned inspection.

- **Predictive Maintenance**: one of the main objectives of the digital twin is predictive maintenance. Early fault detection, identification and prediction will help reduce downtime by converting unscheduled inspection into a scheduled inspection.

- **Cloud Thermal Management System**: the thermal prediction models developed in the project will improve the thermal performance of the powertrain by reducing the losses.

3.5.5 SUMMARY OF POTENTIAL PARAMETERS TO BE MONITORED

Next table includes a preliminary summary of potential parameters and variables to be monitored using IOTP to feed the different algorithms and data analytics systems that will provide advance functionalities related to fault diagnosis and predictive maintenance. Note that not all of these parameters need to be measured, some can be estimated.

Table 3.8. Preliminary list of parameters to be monitored.

Sub-system	Parameters
Power converter	Input Voltage
	Input Current
	Input Power
	Output Voltage
	Output Current
	Output Power (estimated)
	Switching frequency
	Temperature @ power modules
Integrated Motor Drive	Phase
	Output Power (estimated)
	Frequency
	R.P.M
	Torque (estimated)
	Vibrations
	Inner Temperature
	Case Temperature
Thermal system	Heatsink temperature

4 THERMAL SPECIFICATIONS

This section describes the thermal specifications of the designed power converter. The cooling system must refrigerate the power converter and the motor, so it should consider the losses of both elements.

In order to study which dissipation systems are suitable for the project, we must consider different factors. Firstly, we need to define some environmental conditions, such as ambient temperature, relative humidity, altitude of the driving, etc. The converter designed in the RHODaS project should only be used in environments that meet these specifications. These conditions will affect the operation of the converter, its losses, design, and the dissipation system. Table 4.1 shows the different environmental specifications.

Table 4.1. Environmental specifications

Parameter	**Value**
Ambient temperature range	From -20 ºC to 50 ºC
Altitude	Up to 2000 m
Maximum relative humidity	90%

Moreover, knowing the system losses is necessary to design the dissipation system. Ideally, the converter should have an efficiency of 97 %. However, the efficiency—and therefore the losses—depends on factors such as ambient temperature, dissipation system, switching frequency, converter power and semiconductors. In addition, the motor also influences the total system losses.

In order to have an approximate value of losses and compare them with the theoretical value, a simulation of the converter is performed. A hybrid converter with GaN in parallel (see Figure 3.4) is analysed, and a silicon carbide converter (see Figure 3.6) could be also studied. Both converters work at 80 kHz and provide a power of 100 kW. The junction temperature of the devices is 90 ºC. In addition, the motor efficiency is 96 %. Table 4.2 shows the results obtained.

Table 4.2. Simulated power converter losses

Power converter	**Converter efficiency**	**Converter losses**	**Motor efficiency**	**Motor losses**	**Total losses**
Ideal	97.00 %	3.00 kW			7.00 kW
Hybrid GaN-SiC	97.30 %	2.70 kW	96 %	4 kW	6.70 kW
Full-SiC	96.17 %	3.83 kW			7.83 kW

In view of the above results, the dissipation system should be able to dissipate about 7 kW or 8 kW. This value is indicative and should be recalculated when the converter components and their operation are fully defined.

4.1 COOLING SYSTEMS

The cooling mechanism of an inverter is required to maintain the junction temperature of the semiconductor devices during the operating conditions. This demands efficient usage of the resources. The cooling mechanism for automotive vehicles are available in different designs implemented with separate cooling techniques (Figure 4.1). There are inverters that are gas-cooled [1], however, the basic approach considered for inverters is air and liquid cooling. For RHODaS, liquid cooling has been given prime focus.

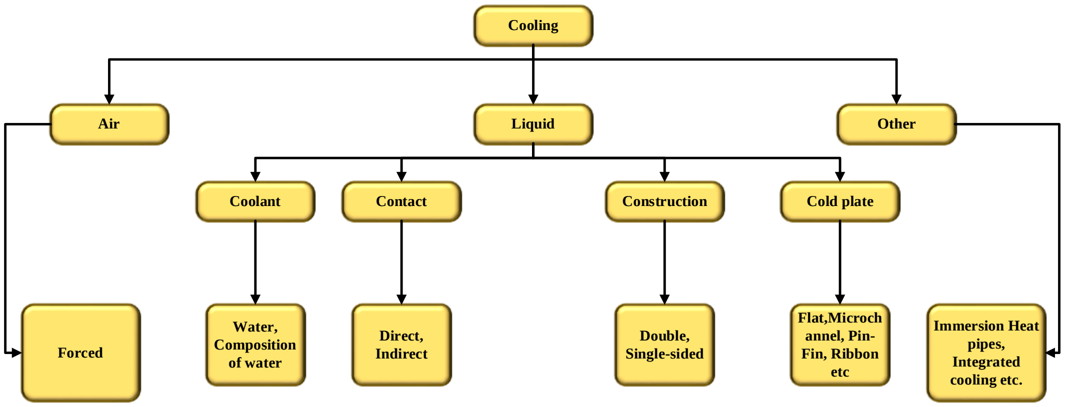

Figure 4.1 Classification of cooling techniques for automotive inverters

4.1.1 Liquid Cooling

Despite the convenience of air-cooling, liquid cooling is usually chosen as the best option for EVs for its higher thermal transfer capability. Furthermore, with respect to the cost and design of the system, liquid cooling is justified to be more effective [2]. Indirect liquid cooling using a cold plate is considered as a conventional approach with Rth≥ 0.8 K/W. However, the direct approach with complex cold plates is weighed as a more advanced structure with better thermal performance. By introducing direct cooling, power module layers could be reduced which also reduces the thermal resistance by up to 30% [3].

Among multiple direct cooling structures, jet impingement (0.44–0.48 K/W), turbulator (0.2–0.55 K/W), and microchannel (0.13–0.24 K/W) technologies can be distinguished as major schemes [4]. With a more complex design structure, the cost factor also increases and this only justifies when higher thermal performance is required.

Single-Sided Direct Liquid Cooling

Single sided liquid cooling is the most well-known and cost-effective solution for automotive inverters. Currently, the indirect liquid cooling is being offered in new structural designs of cold plates and heat sinks. In [5], a heat sink with regular pin fins cooling channels is introduced. Another common approach is a cold plate for WBG inverters with a pin fin structure [6]. In [7], a 30 kVA SiC inverter is investigated with a liquid cold plate for a high-temperature operation range. The junction temperature was 150°C and the ambient temperature was 180°C. For which the temperature of cold plates and coolant were 85 and 50°C, respectively. Another SiC-based 100kW inverter is tested in [8] with a flat cold plate at 105°C ambient and 65°C coolant temperatures. In [9], a 125kW inverter is investigated with the two-level liquid-cooled cold plates (Figure 4.2). The two cold plates are utilized to cool the power modules and the DC link bus from the sides. Another example is discussed in [10], where a power module of six different SiC devices was presented with a thermal resistance of 0.331K/W.

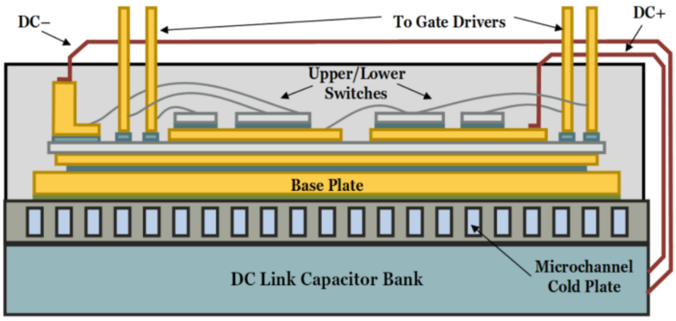

Figure 4.2 Principle of the two-sided cold plate for a module and DC link capacitors cooling

An automotive 1200V 150A inverter with an indirect liquid mixture of 50/50% water/glycol with a copper heat sink of round pins was also investigated. Parallel SiC devices were used with a 1mm distance between them. Simulated results showed the chip temperature was reduced from 226 to 154°C, where the maximum allowed junction temperature of the module was 170°C. The hotspot temperature was further improved by changing the inlet liquid flow and temperature and as a result, the thermal resistance was reduced to 32.1% [12].

Double-Sided Liquid Cooling

This scheme is usually applied for motor drives applications. For example, in [13] and [14] double sided cooling is presented with jet impingement. Another investigation is carried out in [15], double-sided cooling concept is proven on a half-bridge power module (Figure 4.3). For the performance comparison between the single and double-sided cooling schemes, a wide range of boundary conditions was set and thermal resistance was calculated. From the results, the double-sided scheme offers lower thermal resistance of up to 70% only when a high heat transfer coefficient is achieved, i.e. h > 106 W/(m^2 ·K) with an AlN type substrate. This substrate is costly but chosen when high thermal efficiency is required.

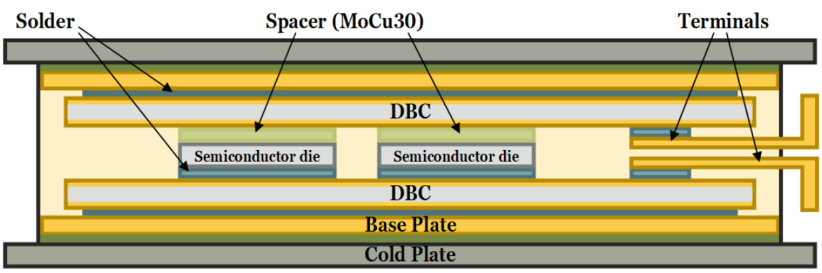

Figure 4.3 Schematic double-sided module representation

Another case is discussed in [16] where a full bridge inverter is considered with double-sided liquid cooling. Results showed 35% reduction in the thermal resistance with a final value about 0.175 K/W. It also provided a solution for situations when parallel connection of semiconductor devices is required for sharing large output currents. The imbalance of currents is quite considerable at high switching frequencies in almost all interconnections. An embedded chip is also introduced to provide linear currents by reducing the deviations from 10% to 2%. Eventually, the design was able to reduce the power losses by 60% in comparison to single-sided cooling scheme.

Single-sided indirect cooling is considered to be the most feasible mode of cooling scheme for power electronics application, especially in EVs. However, there is still a room for improvement by improving the cold plates [6]. The single-sided direct and indirect cooling for WBG devices can be optimized by either tweaking the space between the chips or by altering the number of power switches [12]. The WBGs offer small chip-size which also allows additional parallel-connected power switches for better current sharing. From a thermal efficiency point of view, small chips enable a large distance between the switches which assures better temperature distribution and heat dissipation capability. Larger spacing between semiconductors may on the other hand lead to a lower power density.

For single-sided cooling, higher rated current WBG semiconductors are required for optimized performance. Double-sided cooling may be more reliable due to the potential availability of more reliable interconnectors instead of bonding wires. Furthermore, the double-sided approach could be implemented for optimized current flow between the parallel modules. Although double-sided cooling presents promising thermal performance with reduced thermal resistance of up to 35%, its dissipation capability is still low and does not justify its complex implementation [14].

4.1.2. Description of proposed thermal management system

The TMS needs to ensure that the thermal limits are kept and will do so by actively controlling the pump motor(s). The power to and from the inverter is also monitored and will be used to calculate lifetime and loading. The current control of the inverter should be able to limit the current based on calculations from the TMS to keep the motor and inverter within a thermal envelope. The exact configuration, control objectives, control methodology and test & validation will depend on the final system architecture.
The key features of the TMS are:

- Monitor and measure temperatures to send warning/alarms to the main system control unit.
- Evaluate the thermal loading of the system components regarding the lifetime, using the thermal sensors T and the power sensors P.
- Calculate the maximum power/current under overload conditions for the motor control.
- Ensure the junction temperature of semiconductor devices to not exceed the limit.

The proposed TMS intends to reduce the negative effect of high thermal loading by ensuring sufficient cooling. The cooling is ensured by monitoring the system conditions and using active prediction to limit the thermal loading of the power converter and the aging. Thermal loading may be limited by e.g., changing modulation strategy, motor control method [25], switching frequency or limit the motor current.

The active prediction is based on detailed thermal models of the main components and is evaluated on the fly in the drive. This quasi-real-time detailed thermal model is also used to estimate the remaining useful lifetime of the converter. The needed detail level of the thermal model will be determined based on the tests and the CFD/FEM simulations. The model will be a thermal equivalent circuit model supplemented with needed lookup tables.

A small-scale two-phase cooling system may also be tested. The two-phase cooling can potentially reduce the size and weight of the cooling system. This is considered to be a potential improvement. Different dual-phase materials may be considered and different pumping/valve setups may also be considered.

Due to the high thermal loading of the inverter, the connection to the cold plate becomes critical. This requires a detailed investigation into the required smoothness of the power components and the cold plate. Furthermore, an optimised pattern of the thermal paste also needs to be investigated, together with an investigation of the thermal behaviour of involved materials (thermal expansion/thermal conduction/mechanical contact for power connections).

4.1.3. Cooling design near the power modules

A detailed cooling design requires a detailed and finalized electronic design. Ideally an optimizing design would be an electrical, EMC, and thermal co-design. Due to the high-power density, even minor circuit design changes may have significant impact. Main heat flux will be going through the thermal lowest resistance path and this will for larger modules be the cooling surface designed by the power module manufacturer. Some heat can also be moved through the inverter bus-bars, but this depends on the chosen power modules bonding wire design. There may be limited thermal contact through other surfaces simply due to the potentially higher equivalent thermal resistance. So, the main design challenge would be in designing and optimizing the thermal interface between power module and cold plate and the bus-bars.

Some design choices for the mechanical design may also impact the thermal design. Some auxiliary components may be limited in their thermal rating, e.g., auxiliary switch mode coils, filter capacitors, ceramic resonators/crystals. It may be an advantage to e.g., mount the inverter under the motor with the power modules turning upwards. If the PCB design is made for e.g., pollution degree 4, the inverter may be more open to passive circulation of ambient air.

Finally practical considerations may have an impact. Mounting of power modules is sensitive with regards to e.g., surface roughness, mounting pressure, application a cooling paste pattern. The cooling paste pattern depends on the cold plate design as well as the e.g., mounting holes and mounting force [24]. Often a stencil is used ensure that thermal paste has good contact on the entire surface by have different spacing between as can be seen on Figure 4.4. This pattern depends on choice of modules and the resulting thermal design.

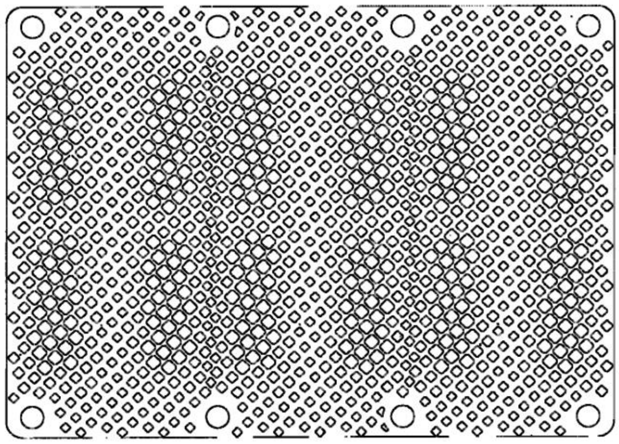

Figure 4.4 Stencil-pattern for application thermal paste [24]

To further optimize the design a finite element design-based optimization will be used to further optimize the thermal design as shown on Figure 4.5. The finite element simulation depends on detailed information regarding module geometry if e.g., junction temperature is to be estimated. To improve estimation of junction temperature a models informed by tests may be needed [23].

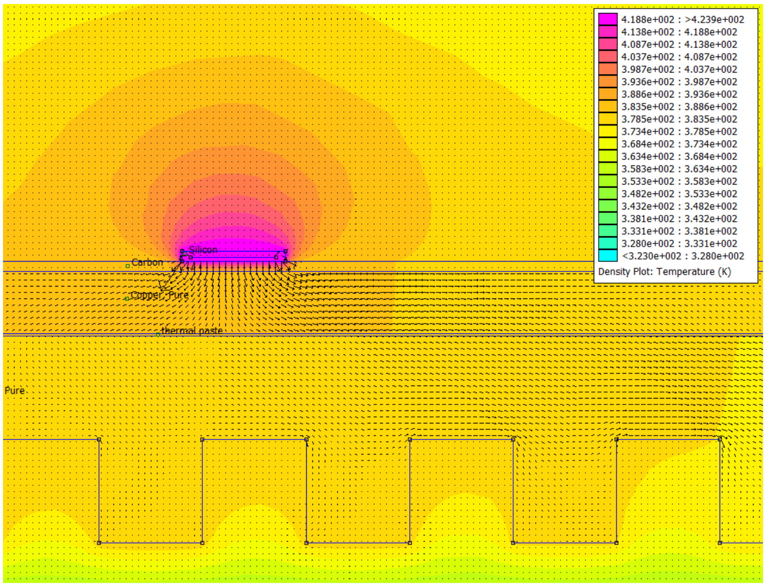

Figure 4.5 Finite element simulation (FEM) of a water-cooled semiconductor with 80C (353 Kelvin) water and 50C (323 Kelvin) ambient air with a finned heatsink design

So, the proposed design procedure is approximately as follows:

- Approximate thermal estimate based on datasheet values to inform the electrical design;
- Based on a more detailed design elaborate the thermal design based on chosen modules;
- Optimize cold plate and thermal fin design based on the more elaborate thermal design using;

- Test thermal design using first power resistors as proxy for the power modules;
- Evaluate the thermal design of the PCB and connectors using FEM simulations and measurements on the actual PCB; and
- Optimize thermal paste stencil on finalized circuit design with actual power modules.

This will be done on the high-power prototype.

4.1.4. Preliminary size estimation

To get an idea of the approximate surface area need for cooling, the power losses from Microchip MSCSM120AM042CT6LIAG power module is used to estimate the possible thermal flux that is possible through a given surface area (see Appendix B).

Using this number and the module height specificized in Appendix B it is possible to obtain a possible preliminary surface area estimation under two cases: with 250 kW overload capacity and 150 kW absolute maximum capacity seen in figures below. They both demonstrate the correlation between efficiency and size.

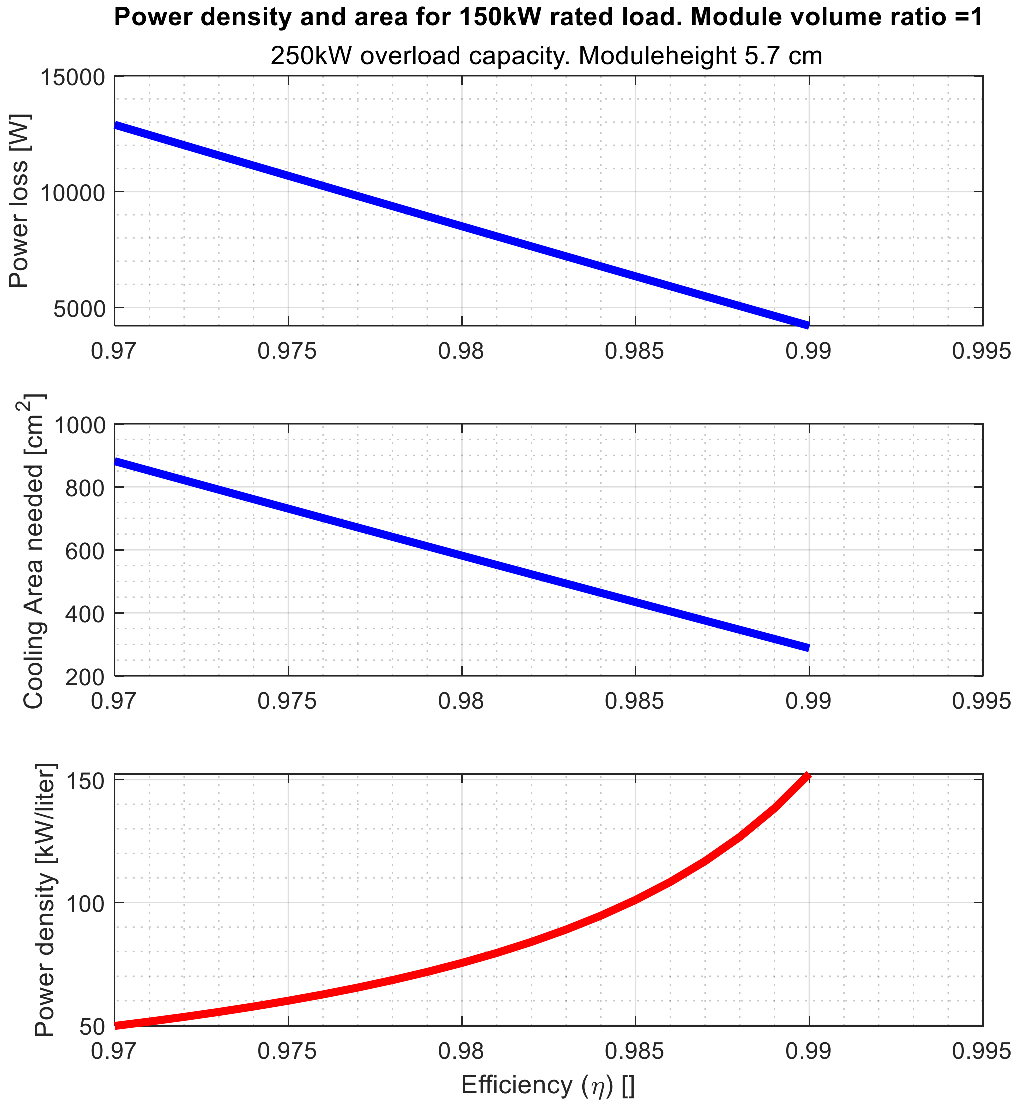

Figure 4.6 With 250 kW overload capacity the surface area and power density as a function of efficiency

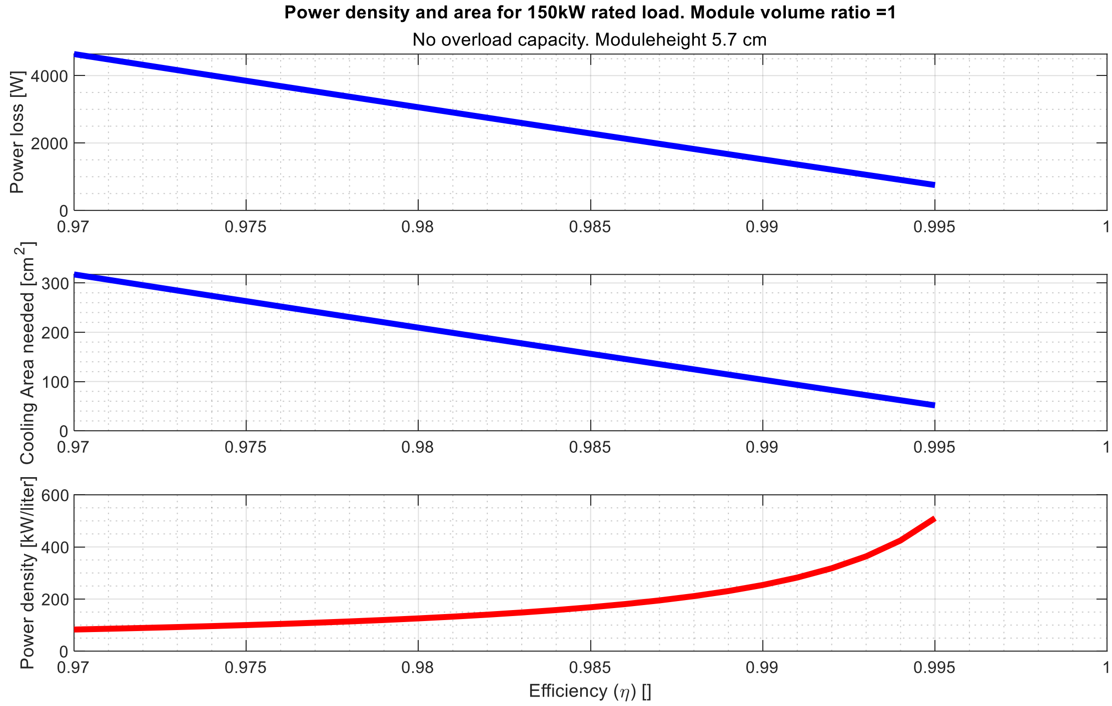

Figure 4.7 With 150 kW maximum capacity the surface area and power density as a function of efficiency

4.2 THERMAL SPECIFICATIONS

Table 4.3 summarizes the environmental specifications detailed in this section for the power converter. Moreover, the table presents the specifications for the cooling system.

Table 4.3. Summary of the thermal specifications

Parameter	**Value**
Ambient temperature range	From -20 ºC to 50 ºC
Altitude	Up to 2000 m
Maximum relative humidity	90%
Power to be dissipated[1]	Estimation: 3 kW from the converter and 6 kW from the motor.
Cooling system	Glycol + water for cooling the inverter
Surface area needed for 150kW with no overload at 97.5% efficiency[2]	263 cm^2

[1]These values depend on the losses from the power converter and depends on achieved efficiency and power needed.

[2]With a converter height of 57 mm this gives approximately, 100kW/L (assumes no spacing between power modules). The final implementation geometry should accommodate the cooling needs.

5 CONCLUSION

This deliverable presents the specifications and requirements for the electrical and electronic system of the RHODaS project converter. Additionally, it also addresses initial thermal system requirements and possible solutions for it.

The deliverable describes the requirements of the electromechanical system, i.e., the converter and motor assembly. It defines the possible size of the converter depending on the rated power. The preliminary dimensions of the 150 kW converter are 210 × 380 × 30 mm (length x width x height). These dimensions comply with the desired power density of 100 kW/L since the converter can deliver a peak power of 250 kW. The final dimensions of the converter, IMD and integrated system specifications shall be performed in Task T5.5 and presented in D5.4 (M42), as detailed in the DoA.

Regarding electronic requirements, the converter is a modular T-type built with SiC and GaN devices. Top and bottom transistors will be SiC MOSFETs, while the two transistors connected to the midpoint of the DC bus will be GaN e-HEMTs. The converter should be modular so that the power can be scaled if necessary. Consequently, each module will consist of one phase of the converter with its respective sensors and DC bus capacitors.

Since the converter must be able to handle nominal powers of 150 kW, with voltages around 1000 V, it must support currents of 150 A (rms). Commercially available GaN devices can only withstand low voltages (< 650 V) and currents, so it may be necessary to look for alternatives. The optimum alternative is to use GaN module prototypes provided by GaN Systems able to withstand high currents, Additionally, it also addresses the thermal system requirements. An interesting proposal is to parallelize GaN transistors to work with higher currents. Other proposals are to operate the power converter on two level-three level control according the currents required, to develop specific switching patters and to lower the converter operating voltage. The ultimate containment plan is to build a SiC-only converter. This last proposal will only be made if all others are unfeasible. The switching frequency should be between 50 and 100 kHz and has to be adjusted to reach a balance between losses, EMI and output current quality.

Finally, there is the thermal management system. The design of the cooling system depends on the conditions of use of the converter. Therefore, these conditions are defined. The usage temperature ranges from -20 °C to 50 °C. The maximum relative humidity is 90%, and the maximum altitude of use is 2000 m. The precise power losses will be determined before the final cooling sizing is determined, but the inverter cooling is sized approximately at 3 kW (water + glycol cooling) and the motor losses are estimated for 6 kW (oil cooling).

Being the main objective of this project, Table 5.1 summarizes all the 150 kW power converter specifications detailed in this deliverable.

Table 5.1. Summary of the power converter specifications

Parameter	
Length	210 mm
Width	380 mm

Parameter	
Height	30 mm
Power density	104 kW/L
Maximum efficiency	> 97 %
DC bus voltage	1000 V
Rated power	150 kW
Maximum power	250 kW
Semiconductor	GaN + SiC
Topology	T-type (modular)
Switching frequency	50 – 100 kHz
Rated current (rms)	150 A
Peak current (rms)	250 A
Ambient temperature range	From -20 ºC to 50 ºC
Altitude	Up to 2000 m
Maximum relative humidity	90%
Power to be dissipated	3 kW from inverter and 6 kW from motor at 150 kW inverter output power
Cooling system	Liquid (initial proposal subject to optimization water + 34% Propylene glycol)

REFERENCES

[1] Chinthavali, M.S. Gas Cooled Traction Drive Inverter. U.S. Patent 9,320,179, 3 September 2013.

[2] Uhlemann, A.; Hymon, E. Directly Cooled HybridPACK Power Modules with Ribbon Bonded Cooling Structures. In Proceedings of the PCIM Europe 2018; International Exhibition and Conference for Power Electronics, Intelligent Motion, Renewable Energy and Energy Management, Nuremberg, Germany, 5–7 June 2018; pp. 1–6.

[3] Wang, Y.; Dai, X.; Liu, G.; Wu, Y.; Li, D.; Jones, S. Integrated Liquid Cooling Automotive IGBT Module for High Temperatures Coolant Application. In Proceedings of the PCIM Europe 2015; International Exhibition and Conference for Power Electronics, Intelligent Motion, Renewable Energy and Energy Management, Nuremberg, Germany, 19–20 May 2015; pp. 1197–1203.

[4] Yin, S.; Tseng, K.J.; Zhao, J. Design of AlN-Based Micro-Channel Heat Sink in Direct Bond Copper for Power Electronics Packaging. Appl. Therm. Eng. 2013, 52, 120–129.

[5] Mademlis, G.; Orbay, R.; Liu, Y.; Sharma, N.; Arvidsson, R.; Thiringer, T. Multidisciplinary Cooling Design Tool for Electric Vehicle SiC Inverters Utilizing Transient 3D-CFD Computations. eTransportation 2021, 7, 100092.

[6] Olejniczak, K.; Flint, T.; Simco, D.; Storkov, S.; McGee, B.; Shaw, R.; Passmore, B.; George, K.; Curbow, A.; McNutt, T. A Compact 110 KVA, 140 ◦C Ambient, 105 ◦C Liquid Cooled, All-SiC Inverter for Electric Vehicle Traction Drives. In Proceedings of the 2017 IEEE Applied Power Electronics Conference and Exposition (APEC), Tampa, FL, USA, 26–30 March 2017; pp. 735–742.

[7] Qi, F.; Wang, M.; Xu, L. Investigation and Review of Challenges in a High-Temperature 30-KVA Three-Phase Inverter Using SiC MOSFETs. IEEE Trans. Ind. Appl. 2018, 54, 2483–2491.

[8] Zhang, C.; Srdic, S.; Lukic, S.; Kang, Y.; Choi, E.; Tafti, E. A SiC-Based 100 KW High-Power-Density (34 KW/L) Electric Vehicle Traction Inverter. In Proceedings of the 2018 IEEE Energy Conversion Congress and Exposition (ECCE), Portland, OR, USA, 23–27 September 2018; pp. 3880–3885.

[9] Gurpinar, E.; Wiles, R.; Zhou, F.; Liu, Y.; Dede, E.M. SiC MOSFET-Based Power Module Design and Analysis for EV Traction Systems. In Proceedings of the 2018 IEEE Energy Conversion Congress and Exposition (ECCE), Portland, OR, USA, 23–27 September 2018; pp. 1722–1727.

[10] Huber, T.; Kleimaier, A. Novel SiC Module Design—Optimised for Low Switching Losses, Efficient Cooling Path and Low Inductance. In Proceedings of the CIPS 2018 10th International Conference on Integrated Power Electronics Systems, Stuttgart, Germany, 20–22 March 2018; pp. 571–576.

[11] Abramushkina, E.; Zhaksylyk, A.; Geury, T.; El Baghdadi, M.; Hegazy, O. A Thorough Review of Cooling Concepts and Thermal Management Techniques for Automotive WBG Inverters: Topology, Technology and Integration Level. Energies 2021, 14, 4981. https://doi.org/10.3390/en14164981.

[12] Becker, N.; Bulovic, S.; Bittner, R.; Herzer, R. Thermal Simulation for Power Density Optimization of SiC-MOSFET Automotive Inverter. In Proceedings of the CIPS 2020; 11th International Conference on Integrated Power Electronics Systems, Berlin, Germany, 24–26 March 2020; pp. 1–6.

[13] Liu, C.-K.; Wu, S.-T.; Lo, Y.-Y.; Chiu, P.-K.; Lin, H.-H.; Chen, Y.-S.; Tzeng, C.-M. Double-Sided Cooling SiC Power Module Packaging for Industrial Motor Driving System. In Proceedings of the 2020 15th International Microsystems, Packaging, Assembly and Circuits Technology Conference (IMPACT), Taipei, Taiwan, 21–23 October 2020; pp. 105–108.

[14] Tang, G.; Wai, L.C.; Boon Lim, S.; Lau, B.L.; Kazunori, Y.; Zhang, X.W. Thermal Analysis, Characterization and and Material Selection for SiC Device Based Intelligent Power Module (IPM). In Proceedings of the 2020 IEEE 70th Electronic Components and Technology Conference (ECTC), Orlando, FL, USA, 3–30 June 2020; pp. 2078–2085.

[15] Catalano, A.P.; Scognamillo, C.; Castellazzi, A.; d'Alessandro, V. Optimum Thermal Design of High-Voltage Double-Sided Cooled Multi-Chip SiC Power Modules. In Proceedings of the 2019 25th International Workshop on Thermal Investigations of ICs and Systems (THERMINIC), Lecco, Italy, 25–27 September 2019; pp. 1–4.

[16] Hirao, T.; Onishi, M.; Yasuda, Y.; Namba, A.; Nakatsu, K. EV Traction Inverter Employing Double-Sided Direct-Cooling Technology with SiC Power Device. In Proceedings of the 2018 International Power Electronics Conference (IPEC-Niigata 2018-ECCE Asia), Niigata, Japan, 20–24 May 2018; pp. 2082–2085.

[17] Cheng, C.C.; Chang, P.C.; Li, H.C.; Hsu, F.I. Design of a Single-Phase Immersion Cooling System through Experimental and Numerical Analysis. Int. J. Heat Mass Transf. 2020, 160, 120203.

[18] Birbarah, P.; Gebrael, T.; Foulkes, T.; Stillwell, A.; Moore, A.; Pilawa-Podgurski, R.; Miljkovic, N. Water Immersion Cooling of High Power Density Electronics. Int. J. Heat Mass Transf. 2020, 147, 118918.

[19] Kuncoro, I.W.; Pambudi, N.A.; Biddinika, M.K.; Widiastuti, I.; Hijriawan, M.; Wibowo, K.M. Immersion Cooling as the next Technology for Data Center Cooling: A Review. J. Phys. Conf. Series 2019, 1402, 044057.

[20] Yuki, K.; Kibushi, R.; Tsuji, R.; Takai, K.; Unno, N.; Ogushi, T.; Murakami, M.; Numata, T.; Nomura, H.; Ide, T. Thermal Management of Automotive Sic-Based on-Board Inverter with 500 w/cm2 in Heat Flux, and Two-Phase Immersion Cooling by Breathing Phenomenon Spontaneously Induced by Lotus Porous Copper Jointed onto a Grooved Heat Transfer Surface. J. Therm. Sci. Technol. 2020, 15, 1–11.

[21] Accessed Online [2017]: https://search.abb.com/library/Download.aspx?DocumentID=9AKK107045A6773&LanguageCode=en&DocumentPartId=&Action=Launch

[22] DriveMode project, http://drivemode-h2020.eu/resources/, seen on 13/1 2023

[23] Künzi, R. "Thermal Design of Power Electronic Circuits",reportNumber = "arXiv:1607.01578",2015, CERN Accelerator School Baden, "http://cds.cern.ch/record/2038661", doi = "10.5170/CERN-2015-003.311"

[24], Hitachi application note, "Application Method and Evaluation of Thermal Grease", https://www.hitachi-power-semiconductor-device.co.jp/products/igbt/pdf/application_method.pdf, Seen 14/1 2023

[25], Sidda, Sakunthala & Kiranmayi, R & Nagaraju, P. (2017). A Study on Industrial Motor Drives Comparison and Applications of PMSM and BLDC Motor Drives. 10.1109/ICECDS.2017.8390224.

APPENDIX A – Electronic calculations

This appendix details the calculations performed to obtain some parameters of the high-power converter. First, we set the following parameters:

- Bus voltage (V_{DC}) = 1000 V
- Rated power of the converter: 150 kW
- Maximum power: 250 kW
- Cos(φ) = 0.82

The maximum line voltage at the output of the converter can be calculated using

$$V_{line} = \frac{V_{DC}}{\sqrt{2}} = \frac{1000}{\sqrt{2}} = 707.11 \text{ V}.$$

The current at the output of the converter is determined using the expression

$$I_{rms} = \frac{\sqrt{2} \cdot P}{\sqrt{3} \cdot V_{DC} \cdot \cos(\varphi)}$$

where *P* is the power delivered by the power converter.

Hence, at rated power

$$I_{rms} = \frac{\sqrt{2} \cdot P}{\sqrt{3} \cdot V_{DC} \cdot \cos(\varphi)} = \frac{\sqrt{2} \cdot 150000}{\sqrt{3} \cdot 1000 \cdot 0.82} = 149.36 \text{ A} \approx 150 \text{ A},$$

while at maximum power

$$I_{rms} = \frac{\sqrt{2} \cdot P}{\sqrt{3} \cdot V_{DC} \cdot \cos(\varphi)} = \frac{\sqrt{2} \cdot 250000}{\sqrt{3} \cdot 1000 \cdot 0.82} = 248 \text{ A} \approx 250 \text{ A}.$$

As detailed in Section 2, the GaN e-HEMTs may not be able to withstand 1000 V (500 V). Hence, it may be necessary to lower the bus voltage. Therefore, we repeat the output current calculations for a bus voltage of 900 V.

At rated power

$$I_{rms} = \frac{\sqrt{2} \cdot P}{\sqrt{3} \cdot V_{DC} \cdot \cos(\varphi)} = \frac{\sqrt{2} \cdot 150000}{\sqrt{3} \cdot 900 \cdot 0.82} = 165.95 \text{ A} \approx 170 \text{ A},$$

while at maximum power

$$I_{rms} = \frac{\sqrt{2} \cdot P}{\sqrt{3} \cdot V_{DC} \cdot \cos(\varphi)} = \frac{\sqrt{2} \cdot 250000}{\sqrt{3} \cdot 900 \cdot 0.82} = 276.6 \text{ A} \approx 280 \text{ A}.$$

APPENDIX B – Thermal calculations

A1) Estimation of physical limits to key thermal components in Rhodas

A1.1) Maximum thermal flux through contact surface to cooling plate

To estimate the thermal flux possible through the cooling interface between power module and cooling plate and existing proven design is used as a becnhmark. It should be noted that the losses expected in Rhodas are significantly higher than what normally be expected from power electronics of this power range. This means that non linear effects of the upscaling is not considered in this draft.

Microchip (MicroSemi) MSCSM120AM042CT6LIAG (SiC) halfbridge is used as basis for the calculations.

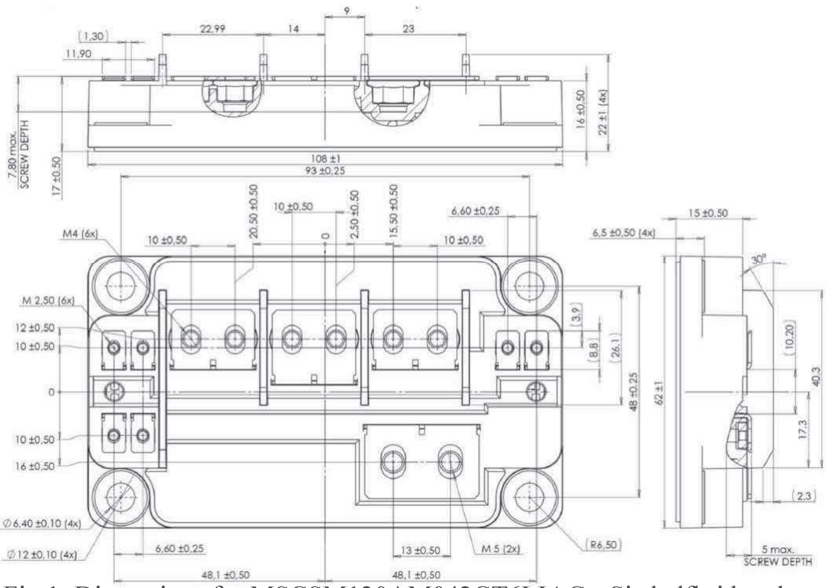

Fig 1: Dimensions for MSCSM120AM042CT6LIAG - Sic halfbridge. length approx. 108mm and width approx. 62mm

$l_{module} := 108\ mm$ $\qquad w_{module} := 62\ mm$

$$S_{hole} := \left(\frac{6.6\ mm}{2}\right)^2 \cdot \pi = 34.212\ mm^2$$

$$A_{cooling\_module} := l_{module} \cdot w_{module} - 4 \cdot S_{hole} = 65.592\ cm^2$$

Maximum transient power loss allowed for this module is 2035W at casing temperature of 25C, with maximum continous operating junction temperature of 150C (transient overload junction max 175C).

Steady state max losses in halfbridge in module due to internal thermal resistance, assuming $T_{case} := 80\ °C$

$T_{junction\_max} := 150\ °C$ $\qquad R_{th\_junction\_to\_case\_1s} := 0.073\ \frac{K}{W}$

$$\Delta T_{worst\_case} := T_{junction\_max} - T_{case} = 70\ K$$

$$P_{worst\_case} := \frac{\Delta T_{worst\_case}}{R_{th\_junction\_to\_case\_1s}} = 958.904\ W$$

Steady state max losses in halfbridge in module due to internal thermal resistance, assuming $T_{case} := 25\ °C$

$$\Delta T_{best\_case} := T_{junction\_max} - T_{case} = 125\ K$$

$$P_{best\_case} := \frac{\Delta T_{best\_case}}{R_{th\_junction\_to\_case\_1s}} = 1.712\ kW$$

Thermal flux is gives a number for power density through the cooling surface.

$$Q_{thermal} := \frac{P_{worst\_case}}{A_{cooling\_module}} = 146.193\ \frac{kW}{m^2}$$

The number of modules need can then be calculated based on the efficiency specified

$\eta := 0.97$ $\qquad P_{out\_max} := 250\ kW$ $\qquad P_{in} := \frac{P_{out\_max}}{\eta} = 257.732\ kW$

$$P_{loss} := P_{in} - P_{out\_max} = 7.732\ kW$$

The area needed keeping the termal flux can the be calculated

$$A_{cooling\_needed} := \frac{P_{loss}}{Q_{thermal}} = 528.886\ cm^2$$

The number of modules needed to distribute these losses:

$$No\_modules := \mathrm{ceil}\left(\frac{A_{cooling\_needed}}{A_{cooling\_module}}\right) = 9$$